Warm measurements on cavities/HOMs

J. A. Mitchell [1, 2]

[1]Engineering Department, Lancaster University

[2]BE-RF Section, CERN

Graeme Burt

Rama Calaga

6th HL-LHC Collaboration Meeting

Espace St Martin, Paris, 14-16 November 2016

Presentation outline

1. HOM coupler test boxes
   - HiLumi HOM couplers
   - RFD single coupler
   - L-bend transmission
   - Coaxial chamber
2. HOM coupler conditioning
3. Longitudinal measurements (DQW)
   - On-axis bead-pull
   - Multipole measurements
   - Stretched wire measurements
4. References

Higher Order Modes (HOMs)

- **Higher Order Modes (HOMs)**
- Modes of operation which occur at frequencies higher than the operational mode.
- If excited by an external source, the HOMs can deviate from the desired crabbing operation.

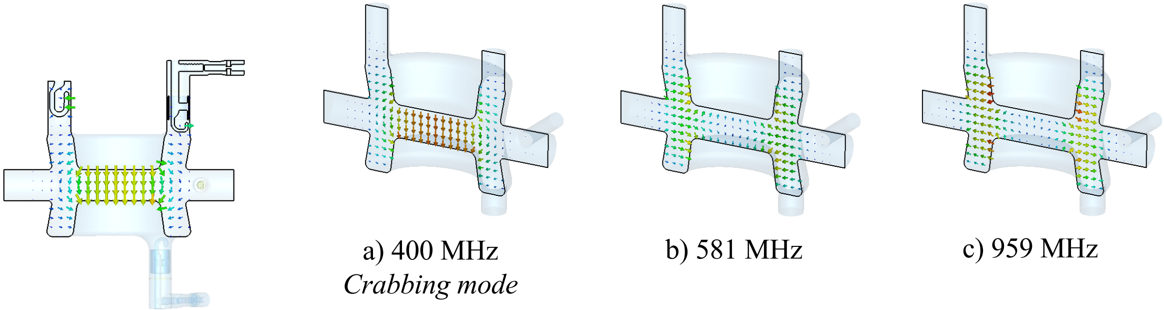

a) 400 MHz *Crabbing mode* b) 581 MHz c) 959 MHz

- HOM couplers damp the higher order modes to a load but whilst acting as a stop-band filter for the crabbing mode at **400 MHz**.

HiLumi crab cavity HOM couplers

- The two HiLumi crab cavities to be tested in the SPS in 2018 are the Double Quarter Wave (DQW) and Radio Frequency Dipole (RFD).
- Each has HOM couplers with associated spectral responses tailored at providing a path at the HOM frequencies but acting as a stop-band to the crabbing mode.

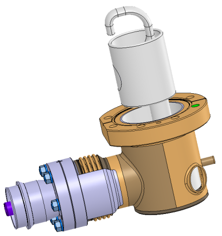

a) SPS DQW HOM coupler

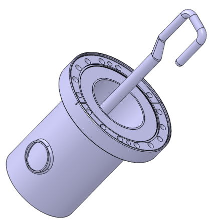

b) RFD HOM coupler

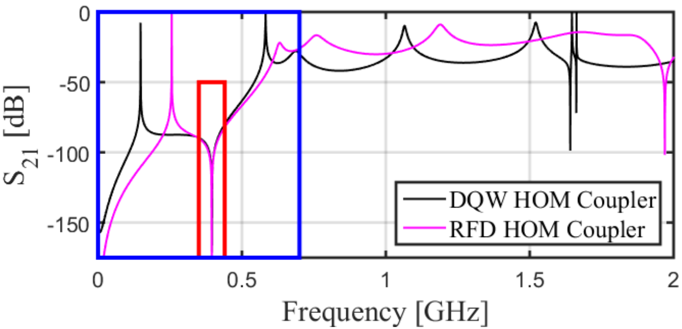

c) Spectral responses of the HOM couplers

- It is beneficial to know the **spectral response** of the HOM couplers **pre-installation**.

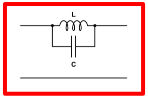

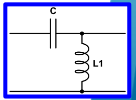

Note: DQW HOM coupler design alterations have been applied for the LHC design by B. Xiao.

DQW L-bend transmission test box

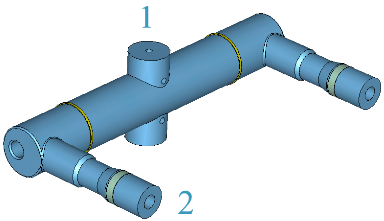

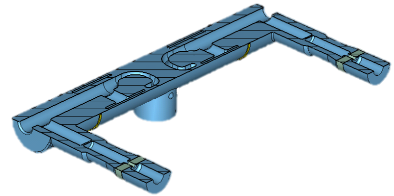

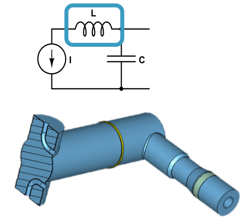

- Uses probes which preferentially use magnetic coupling to couple to the TE110 waveguide mode in order to measure the spectral response.
- 2-port
  - Improves similarity of spectral response to that of the HOM coupler.
  - Allows the feasibility of high power conditioning to be investigated.

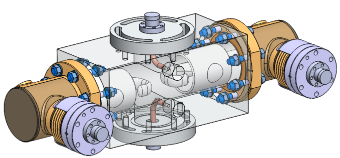

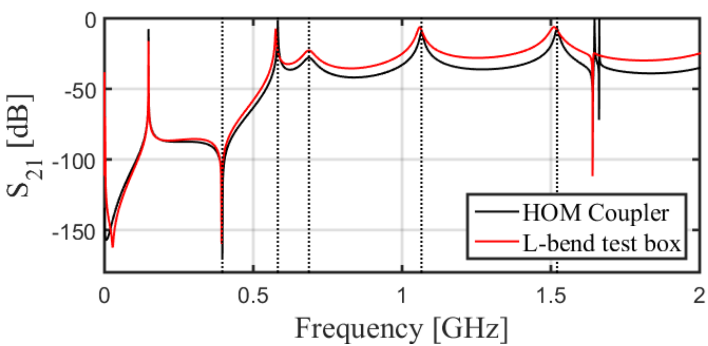

[1]

DQW coaxial chamber test box

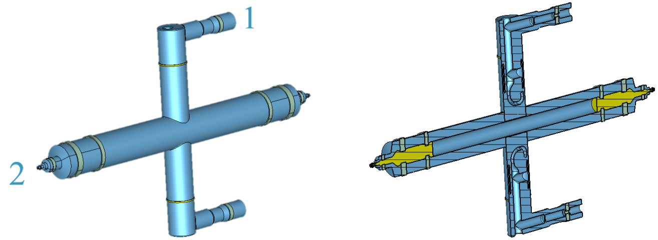

- Uses a **procured** coaxial line and connectors - reduction to 7-16/N-type.
- Peak frequencies not as accurate as L-bend, however simpler manufacture using procured components with documented operational tollerences.
- 2-port
  - Improves similarity of spectral response to that of the HOM coupler.
  - Allows the feasibility of high power conditioning to be investigated.

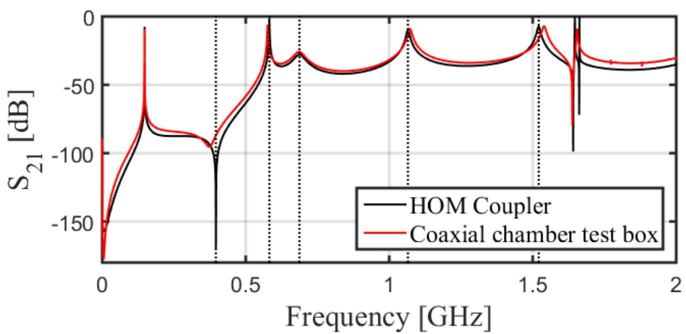

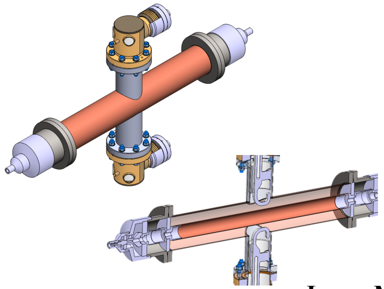

[1]

James Mitchell
j.a.mitchell@lancaster.ac.uk – 15/11/16

DQW test box manufacture

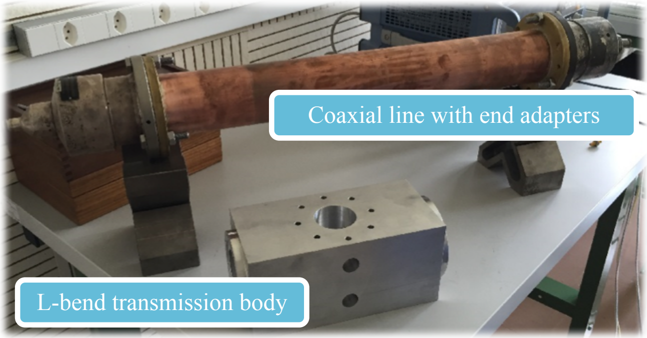

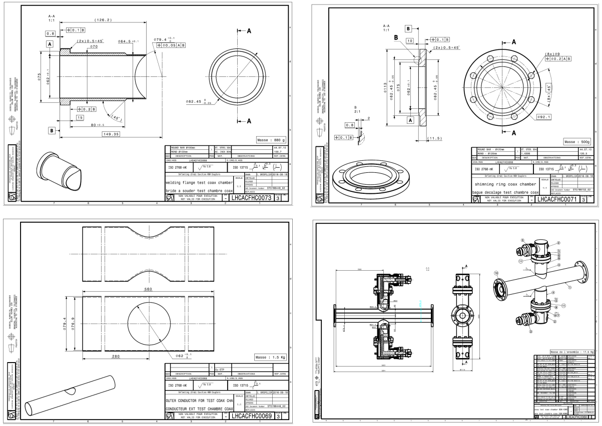

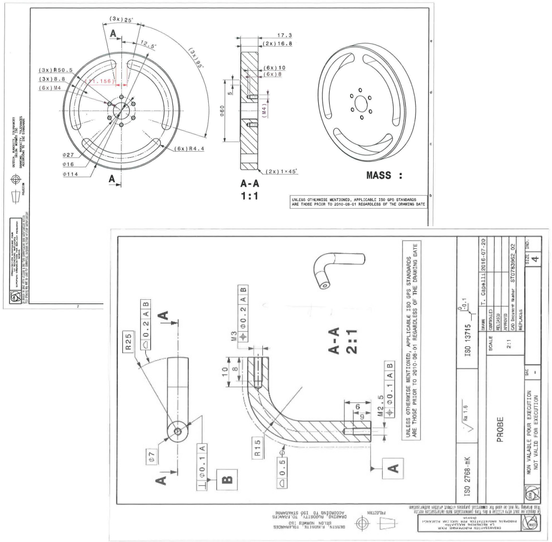

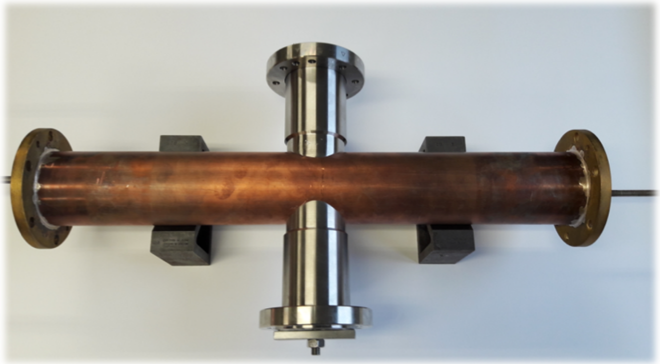

James Mitchell – j.a.mitchell@lancaster.ac.uk – 15/11/16

Coupler conditioning

- As the HOM couplers for the DQW are 'on-cell' there are areas of high field on the coupler surfaces.
- These areas can cause breakdown and heating of the HOM couplers.
- Hence, a device which can pre-condition the couplers prior to installation would be very valuable.

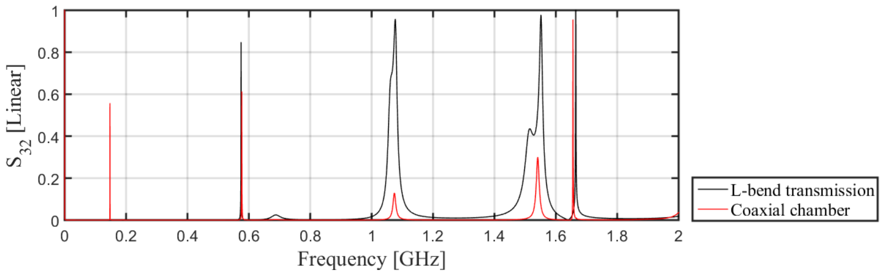

- In both cases, high transmission occurs at the frequencies of the HOM coupler interaction points.
- Areas of high field (i.e. deflecting mode and low Q_{ext} HOMs) should be investigated and the best conditioning configuration can be resulted.

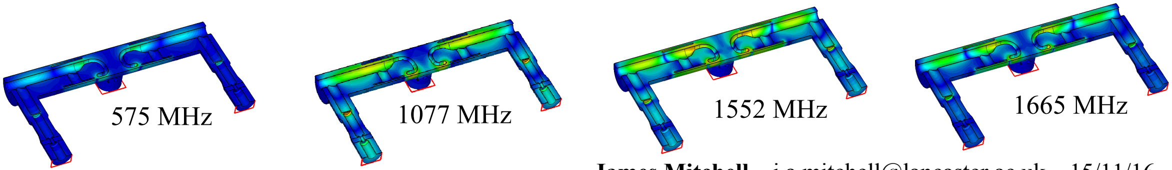

RFD single coupler test box

- For the RFD HOM coupler, a single probe test box has been designed.
- The structure's aim is to accurately **characterise the frequency** of the **stop-band filter**.
- To provide an accurate reference for the frequency of the stop-band, mesh convergence was necessary.

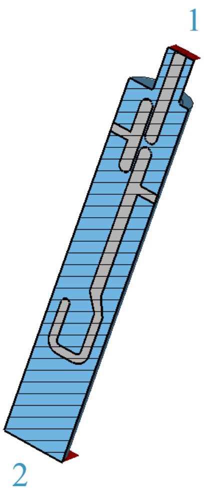

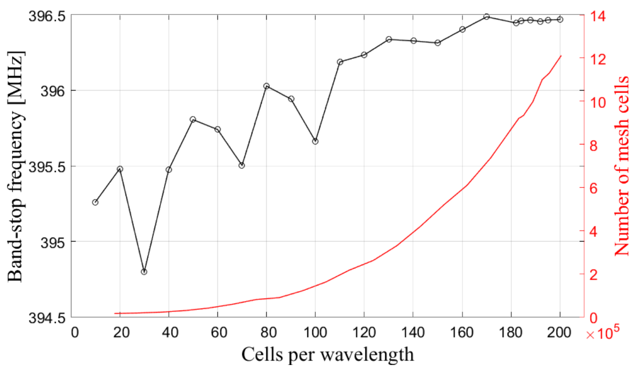

Peak	Frequency [MHz] (3dp)
1	*255.840*
2 (B-S)	**396.487 ± 0.050**
3	*631.020*
4	*759.220*
5	*1189.000*

RFD single coupler test box

- Inductive connection to the wall of the waveguide is needed to diminish the TM_{010} waveguide mode and measure the response of the TE_{110} mode.
- The orientation of the pick-up also effects which waveguide mode is induced.

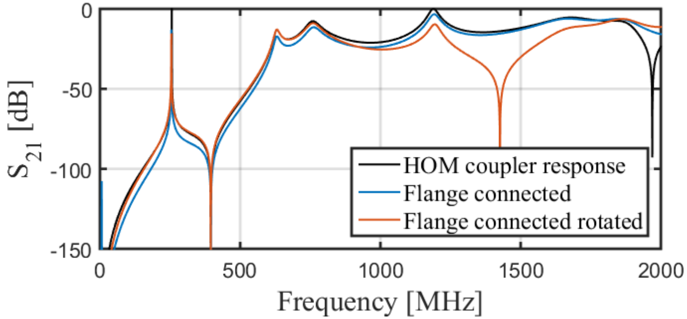

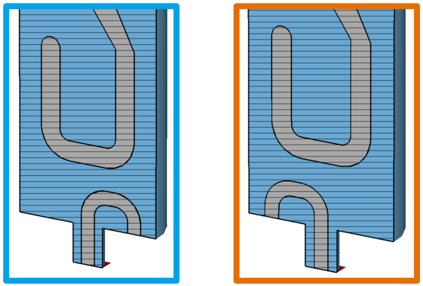

Peak	RFD HOM coupler frequency [MHz] (3dp)	Flange connected [MHz] (3dp)	Flange connected rotated [MHz] (3dp)
Stop-band	396.487 ± 0.050	396.567	396.443

RFD test box manufacture

- Manufacturing drawings are currently being finalised.

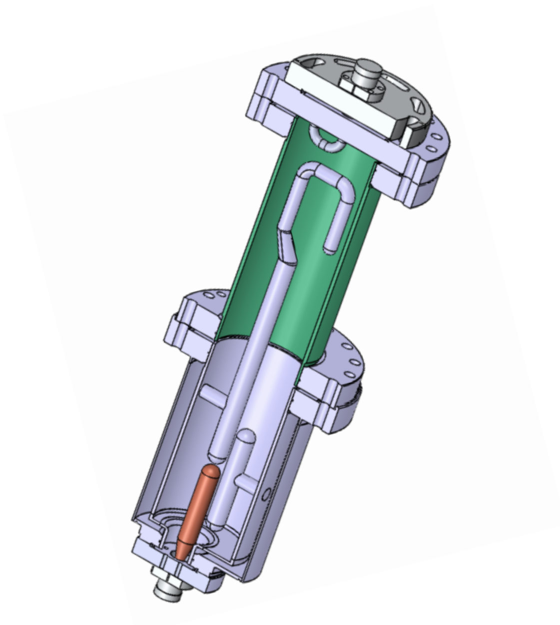

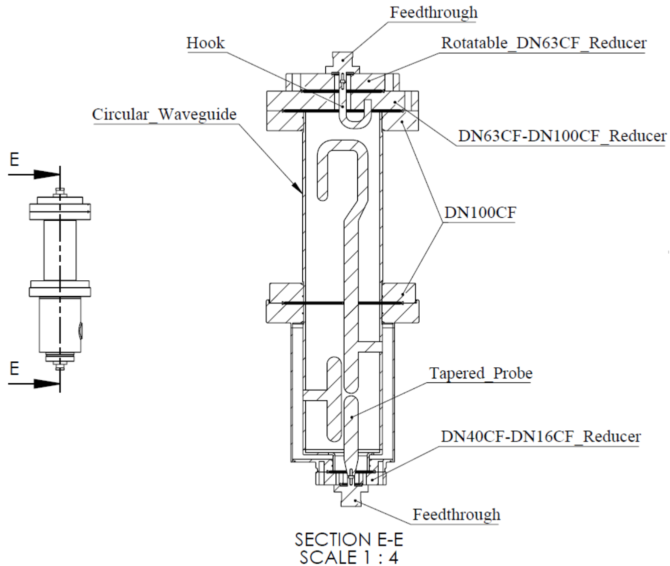

Longitudinal measurements

- **Bead-pull**
  - On axis measurements to result in electric and magnetic field profiles.
  - Azimuthal measurements to try and quantify multipole components.
- **Stretched wire**
  - Allows the electrical centre to be established.
  - This data could then be referenced to the flange geometry for initial calibration.

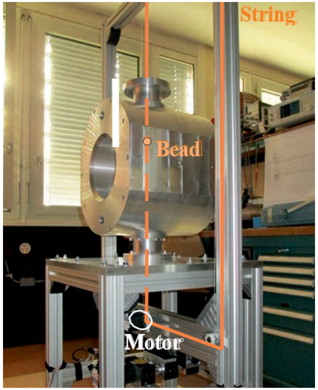

b) Multi-axis bead-pull set-up

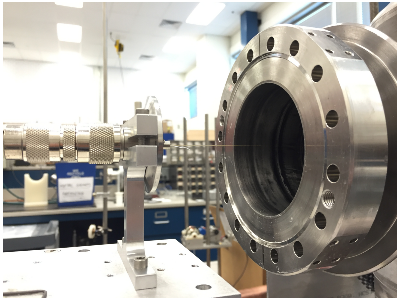

b) Stretched wire set-up at JLAB

On-axis bead-pull

- 3-axis bead-pull set-up.
- Currently an **aluminium machined DQW PoP prototype** is being used to establish techniques **before analysing the Niobium cavities**.
- Metallic and dielectric beads allow electric and magnetic field profiles to be calculated.

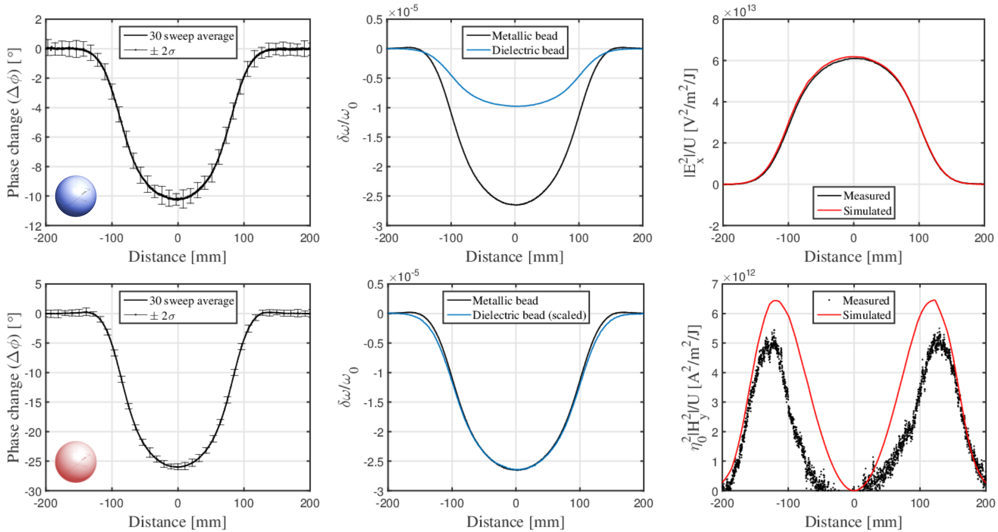

<u>Peak Value ratio (measured/simulated)</u>

98.8%

85.2%

Multipoles

- Multipole components can be calculated using a discrete number of longitudinal electric field profiles over an azimuth.
- Panofsky-Wenzel field decomposition can be used to calculate the multipole coefficients [2].

$$a_n = \frac{jn}{\omega\pi}\int_{-\pi}^{\pi}\frac{1}{r^n}sin(n\theta)\int_{-l/2}^{l/2}e^{\left(\frac{j\omega z}{c}\right)}E_z(r,\theta,z)\;dzd\theta \quad (1)$$

$$b_n = \frac{jn}{\omega\pi}\int_{-\pi}^{\pi}\frac{1}{r^n}cos(n\theta)\int_{-l/2}^{l/2}e^{\left(\frac{j\omega z}{c}\right)}E_z(r,\theta,z)\;dzd\theta \quad (2)$$

- Where n is the multipole number, i.e. n = 0 is the monopole, 1 is the dipole and 2 the quadrupole etc.
- r represents the radius at which the azimuthal integration takes place, z is the position along the longitudinal axis and Ez is the longitudinal electric field.

Multipole simulations

- In order to calculate the multipoles from simulation, a discrete number of longitudinal electric field profiles are taken over an azimuth at a specific radii.
- For visualisation of the multipole kicks, the field can be decomposed into E_{acc} for each of the multipole components.

$$E_{acc} = e^{\left(\frac{j\omega z}{c}\right)} E_z(r, \theta, z)$$

$$E_{acc}^{(n)} = j \int_{-\pi}^{\pi} \frac{1}{r^n} cos(n\theta) E_{acc} \, d\theta$$

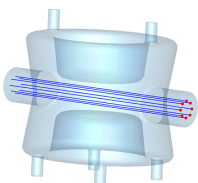

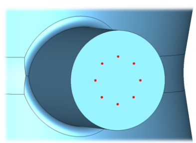

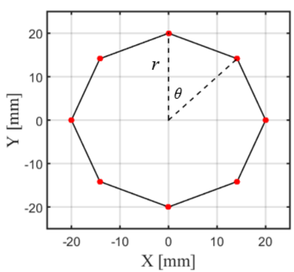

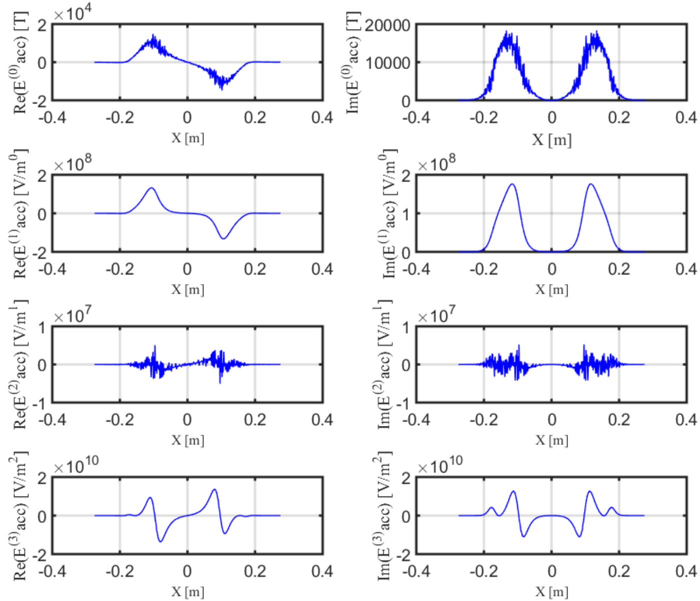

Normalised to 1J of stored energy in the cavity.

Multipole simulations

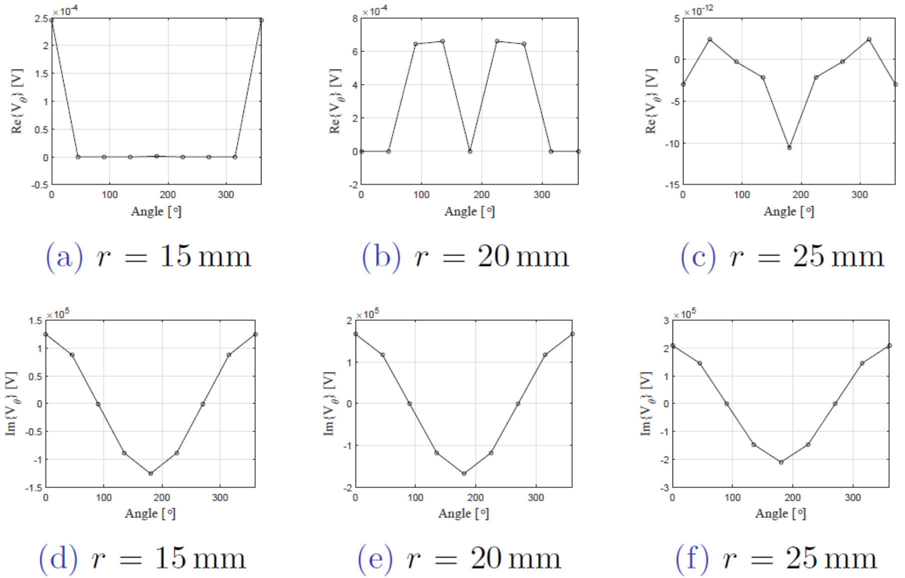

(a) $r = 15\,\mathrm{mm}$ (b) $r = 20\,\mathrm{mm}$ (c) $r = 25\,\mathrm{mm}$

(d) $r = 15\,\mathrm{mm}$ (e) $r = 20\,\mathrm{mm}$ (f) $r = 25\,\mathrm{mm}$

	b_0	b_1	b_2	b_3
Re{b_n}	0.00E+00 ± 0.00	-3.33E+01 ± 1.74E-03	1.77E-01 ± 6.53E-02	-1.04E+03 ± 2.27E-01
Im{b_n}	0.00E+00 ± 0.00	1.01E-08 ± 3.26E-08	-1.41E-06 ± 4.47E-06	-1.89E-04 ± 1.76E-04

Multipole measurements

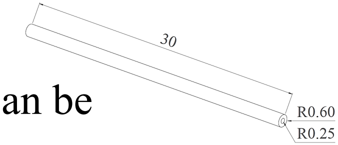

- By using a metallic needle the electric field on axis can be determined via bead-pull measurements.
- Following this, the same mathematics can be applied for multipole analysis.
- Initially this was trialled with a 30 mm needle at three radii with 8 points along the azimuth.

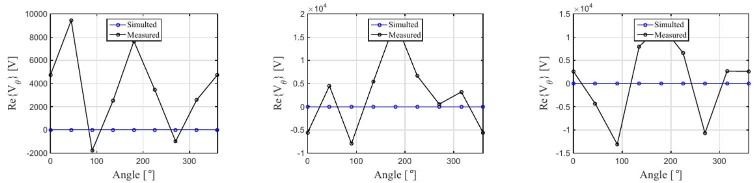

(a) $r = 15\,\mathrm{mm}$ (b) $r = 20\,\mathrm{mm}$ (c) $r = 25\,\mathrm{mm}$

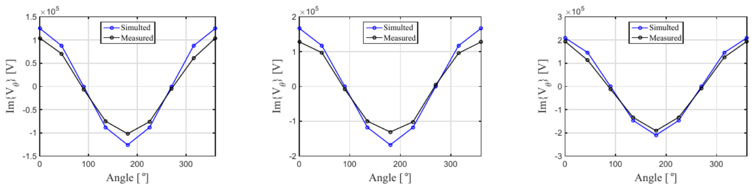

(d) $r = 15\,\mathrm{mm}$ (e) $r = 20\,\mathrm{mm}$ (f) $r = 25\,\mathrm{mm}$

- Imaginary points gave a close representation of the simulated.
- However, difference due to the S/N ratio was too large for meaningful and repeatable multipole coefficients.

Multipole measurements – future…

- Due to the similarity of the simulated and measured results, the feasibility of multipole measurements is shown.
- **Error analysis and propagation** should be applied to all data sets.
- After quantifying the error bars at the voltage stage **signal to noise reduction** techniques should be employed and **repeatability studies conducted**.

- ***Improve the S/N ratio!***
  - ✓ Orientate the pick-up loops at 90 degrees to the magnetic field.
  - Put higher power into the cavity amplifier/use cavity as attenuator.
  - ✓ Simulate over a larger number of points.

… Currently I am analysing a data set of 16 points at a radius of 30 mm with a larger field coupling from the pick-ups… results are looking promising.

Stretched wire measurements

- For DQW-NWV-002, stretched wire measurements were preformed.
- The measurements allow the electrical centre of the cavity to be established [3].
- Using the **deflecting mode it is only possible** to see the centre in the **y-direction** – another mode should be used for the x-direction.

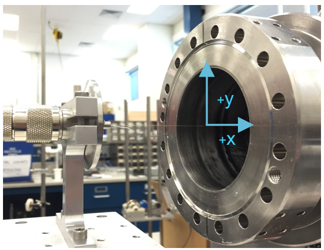

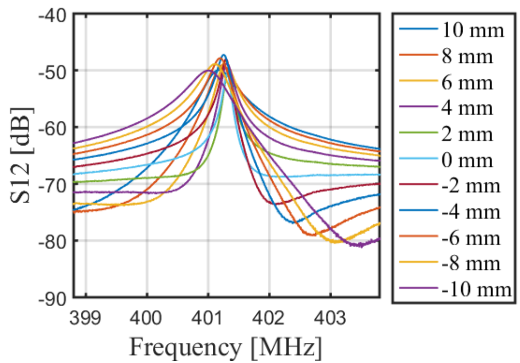

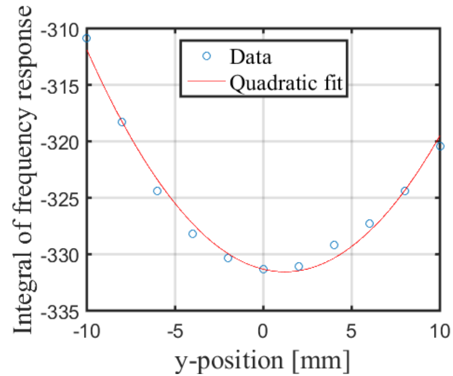

- For the measurements, there is an **observed asymmetry** due to an **impedance mismatch** – this mismatch would have to be eradicated for an accurate fit.
- This technique could be a powerful starting point for calibration to the electrical centre and lends itself well to the multi-axis set-up at CERN.
- To achieve this, **sensitive measurement equipment** should be installed, i.e. opto-couplers, which would allow reference to the geometric map.

References

- J. A. Mitchell. *et al.*
  LHC Crab Cavity Coupler Test Boxes
  in Proc. IPAC16, Busan, Korea, May. 2016, paper WEPMB058, pp. 2248–2250.
- Barranco García, J. *et al.*
  Long term dynamics of the high luminosity Large Hadron Collider with crab cavities
  in Phys. Rev. Accel. Beams, Oct. 2016, Vol 19, Issue 10, pp. 101003–101012.
- Wang, H.
  Wire stretching technique for measuring RF crabbing/deflecting cavity electrical center and a demonstration experiment on its accuracy
  Not yet published.

Special thanks

E. Montesinos
A. Boucherie
T. Capelli
H. Wang